THE JOURNAL OF PHYSICAL CHEMISTRY B

Article

pubs.acs.org/JPCB

# Characterization of KCNE1 inside Lipodisq Nanoparticles for EPR Spectroscopic Studies of Membrane Proteins

Indra D. Sahu, Rongfu Zhang, Megan M. Dunagan, Andrew F. Craig, and Gary A. Lorigan*

Department of Chemistry and Biochemistry, Miami University, Oxford, Ohio 45056, United States

Supporting Information

**ABSTRACT:** EPR spectroscopic studies of membrane proteins in a physiologically relevant native membrane-bound state are extremely challenging due to the complexity observed in inhomogeneity sample preparation and dynamic motion of the spin-label. Traditionally, detergent micelles are the most widely used membrane mimetics for membrane proteins due to their smaller size and homogeneity, providing high-resolution structure analysis by solution NMR spectroscopy. However, it is often difficult to examine whether the protein structure in a micelle environment is the same as that of the respective membrane-bound state. Recently, lipodisq nanoparticles have been introduced as a potentially good membrane mimetic system for structural studies of membrane proteins. However, a detailed characterization of a spin-labeled membrane protein incorporated into lipodisq nanoparticles is still lacking. In this work, lipodisq nanoparticles were used as a membrane mimic system for probing the structural and dynamic properties of the integral membrane protein KCNE1 using site-directed spin labeling EPR spectroscopy. The characterization of spin-labeled KCNE1 incorporated into lipodisq nanoparticles was carried out using CW-EPR titration experiments for the EPR spectral line shape analysis and pulsed EPR titration experiment for the phase memory time ($T_m$) measurements. The CW-EPR titration experiment indicated an increase in spectral line broadening with the addition of the SMA polymer which approaches close to the rigid limit at a lipid to polymer weight ratio of 1:1, providing a clear solubilization of the protein−lipid complex. Similarly, the $T_m$ titration experiment indicated an increase in $T_m$ values with the addition of SMA polymer and approaches ∼2 $\mu$s at a lipid to polymer weight ratio of 1:2. Additionally, CW-EPR spectral line shape analysis was performed on six inside and six outside the membrane spin-label probes of KCNE1 in lipodisq nanoparticles. The results indicated significant differences in EPR spectral line broadening and a corresponding inverse central line width between spin-labeled KCNE1 residues located inside and outside of the membrane for lipodisq nanoparticle samples when compared to lipid vesicle samples. These results are consistent with the solution NMR structure of KCNE1. This study will be beneficial for researchers working on studying the structural and dynamic properties of membrane proteins.

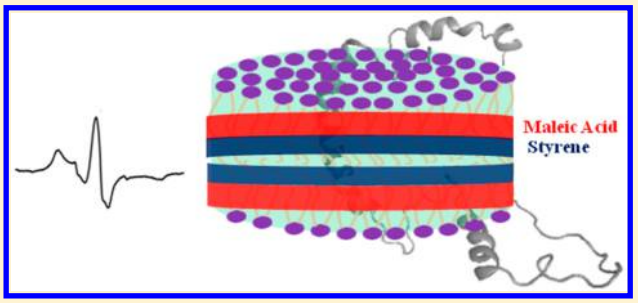


## INTRODUCTION

Membrane proteins play an essential role in controlling bioenergetics, the movement of ions across a cell, and initializing signaling pathways. They are targets of approximately 50% of all modern medical drugs.[1,2] Electron paramagnetic resonance (EPR) spectroscopy is a very powerful biophysical technique for studying the structural and dynamic properties of membrane proteins.[3−5] However, its application is challenging by difficulties in homogeneous solubilization of membrane protein in native membrane-bound state. Detergent micelles are the most widely used membrane mimetics for membrane proteins solubilization due to their smaller size, providing high-resolution structure analysis by solution NMR spectroscopy. However, it is difficult to examine whether the structure of proteins in a micelle environment is the same as that of its membrane-bound state.

Membrane scaffold protein (MSP)-stabilized nanodiscs are a very promising approach to form monodispersed protein samples under lipid bilayer conditions to minimize the detrimental effect of pockets of high local electron spin concentrations on the transverse relaxation within a sample.[6] However, there are drawbacks to this method in that it requires the use of detergents for protein incorporation which must then be completely removed for the assembly of a protein−nanodisc complex.[7] In addition, the absorbance properties of the membrane scaffold protein may interfere with the incorporated protein of interest or there may be specific lipid interactions with the scaffold protein. Finally, they are challenging to prepare.

Bicelles are artificial lipid bilayer discs close to the native mimetic system formed by a mixture of long-chain phospholipids and short-chain phospholipids. Bicelles are favorable for the study of interactions within membrane proteins that are not retained in micelles.[8−11] Bicelles are

Received: February 21, 2017
Revised: May 9, 2017
Published: May 9, 2017





DOI: 10.1021/acs.jpcb.7b01705
J. Phys. Chem. B 2017, 121, 5312−5321

able to provide accessibility for the interaction of both extracellular and cytoplasmic domains of membrane proteins.[12] However, the requirement of the specific types of lipids for the bicelle formation limits its applications as the lipid compositions in the membrane can influence the function of membrane proteins.[12−14]

Lipodisq nanoparticles or styrene maleic acid lipid particles (SMALPs) are a relatively new membrane mimic that can provide a native membrane environment for the structural study of membrane proteins. Unlike nanodiscs, lipodisq nanoparticles are formed from lipids solubilized by polymers instead of membrane scaffold proteins without interfering with the absorbance properties of the membrane proteins.[7,15−18] The formation of lipodisq nanoparticles does not require any detergent. Lipodisq nanoparticles can provide accessibility of the embedded proteins to both sides of the membrane which is appropriate for functional studies.[19] It can maintain the oligomerization states of the proteins which are important for understanding the mechanistic process.[20] The polymer used for solubilizing lipids consists of styrene and maleic acid (SMA) at a molar ratio of 3:1. The SMA copolymer can be applied to a variety of lipids and can maintain the native lipid composition in solubilized nanoparticles.[21−23] Although lipodisq nanoparticles show a high potential to serve as a good membrane mimetic system for biophysical studies of membrane proteins, its structural characterization is still lacking.[15,24]

In this study, lipodisq nanoparticles are characterized in the presence of the integral membrane protein KCNE1. KCNE1 is a single transmembrane protein consisting of 129 amino acids that modulates the function of certain voltage gated potassium ion channels ($K_v$).[25−27] Recent biochemical and electrophysiological studies indicated that the transmembrane domain (TMD) of KCNE1 binds to the pore domain of the KCNQ1 channel modulating the channel's gating.[28−31] Mutations in the genes encoding these proteins result in increased susceptibility to genetic diseases such as congenital deafness, congenital long QT syndrome, ventricular tachyarrhythmia, syncope, and sudden cardiac death.[26,32,33] CW-EPR spectra and transverse relaxation ($T_m$) measurements were conducted on KCNE1 mutants in POPC/POPG lipid titrating with 3:1 SMA polymer for the formation of the lipodisq nanoparticle system. The incorporation of KCNE1 into POPC/POPG lipodisq nanoparticles indicated higher side-chain mobility for the spin-labeled residues located in the aqueous phase when compared to the KCNE1 residues located within the membrane bilayer. The dynamic properties of spin-labeled KCNE1 samples are consistent with the structural behavior of KCNE1. This study provides useful information for researchers using lipodisq nanoparticles as a membrane mimetic system.

## MATERIALS AND METHODS

**Site-Directed Mutagenesis.** The His-tag expression vectors (pET-16b) containing a cysteine-less mutant of KCNE1 were transformed into XL10-Gold *Escherichia coli* cells (Stratagene). Plasmid extracts from these cells were obtained using the QIAprep Spin Miniprep Kit (Qiagen). Site-directed cysteine mutants were introduced into the cysteine-less KCNE1 gene using the QuickChange Lightning Site-Directed Mutagenesis kit (Stratagene). The KCNE1 mutations were confirmed by DNA sequencing from XL10-Gold *E. coli* (Stratagene) transformants using the T7 primer (Integrated DNA Technologies). Successfully mutated vectors were transformed into BL21- (DE3) CodonPlus-RP *E. coli* cells (Stratagene) for protein overexpression. The sites located in the aqueous phase were generated by cysteine substitution corresponding to residues 21, 28, 32, 33, 37, and 109, and the sites located within the membrane bilayer were generated by cysteine substitution corresponding to residues 51, 52, 56, 57, 59, and 63.

**Overexpression and Purification.** The overexpression and purification of *E. coli* BL21 cells carrying mutated KCNE1 genes were carried out by using a previously described protocol.[27] *E. coli* cells carrying mutants of choice were grown in an M9 minimal medium with 50 $\mu$g/mL ampicillin. The cell culture was incubated at 37 °C and 240 rpm until the $OD_{600}$ reached 0.8, at which point protein expression was induced using 1 mM IPTG (isopropyl-1-thio-D-galactopyranoside), followed by continued rotary shaking at 37 °C for 16 h. Purification of KCNE1 from inclusion bodies was carried out according to a previously described method[26] and eluted using 0.05% LMPG detergent. Protein samples were concentrated using a Microcon YM-3 (molecular weight cutoff, 3000) filter (Amicon). The protein concentration was determined from $A_{280}$ using an extinction coefficient of 1.2 mg/mL protein per $OD_{280}$ on a NanoDrop 200c (Thermo Scientific). The protein purity from overexpression was confirmed by sodium dodecyl sulfate polyacrylamide gel electrophoresis (SDS-PAGE).

**Spin Labeling and Reconstitution into Proteoliposomes.** Spin labeling and proteoliposome reconstitution were carried out following the protocol previously described.[34] After purification, each cysteine mutant was concentrated to 0.5 mM and the pH was lowered to 6.5. Samples were then reduced with 2.5 mM DTT, with gentle agitation at room temperature for 24 h to ensure complete conversion to Cys-SH. The MTSL spin label was added to 10 mM from a 250 mM solution in methanol into 0.5 mM KCNE1 solution, which was then gently agitated at room temperature for 30 min, followed by incubation at 37 °C for 3 h and further incubation overnight at room temperature. Samples were then buffer-exchanged into a 50 mM phosphate, 0.05% LMPG, pH 7.8. Following buffer exchange, samples were bound to nickel resin in a column, which was then washed with 200 mL of 50 mM phosphate, 0.5% SDS, pH 7.8, to remove excess MTSL. The spin labeled KCNE1 was eluted using elusion buffer (250 mM IMD, 100 NaCl, 20 mM Tris, pH 7.8) with 0.5% SDS detergent. The spin labeling efficiency (~75%) was determined by comparing the nanodrop UV A280 protein concentration with spin concentration obtained from CW-EPR spectroscopy.

The reconstitution of spin labeled protein into POPC/POPG (3:1) proteoliposomes was carried out via dialysis methods following a similar protocol in the literature.[24,34,35] The concentrated spin labeled KCNE1 protein was mixed with a stock lipid slurry (400 mM SDS, 75 mM POPC and 25 mM POPG, 0.1 mM EDTA, 100 mM IMD, pH 6.5). The lipid slurry was pre-equilibrated to clear mixed micelles via several freeze−thaw cycles. The final protein:lipid molar ratio was set to 1:400. The KCNE1−lipid mixture was then subjected to extensive dialysis to remove all detergent present, during which process KCNE1/POPC/POPG vesicles spontaneously formed. The 4 L dialysis buffer (10 mM imidazole and 0.1 mM EDTA at pH 6.5) was changed twice daily. The completion of detergent removal was determined when the KCNE1−lipid solution became cloudy and the surface tension of the dialysate indicated complete removal of detergent.

**Reconstitution into Lipodisq Nanoparticles.** Lipodisq nanoparticles (prehydrolyzed styrene−maleic anhydride co-



DOI: 10.1021/acs.jpcb.7b01705
J. Phys. Chem. B 2017, 121, 5312−5321

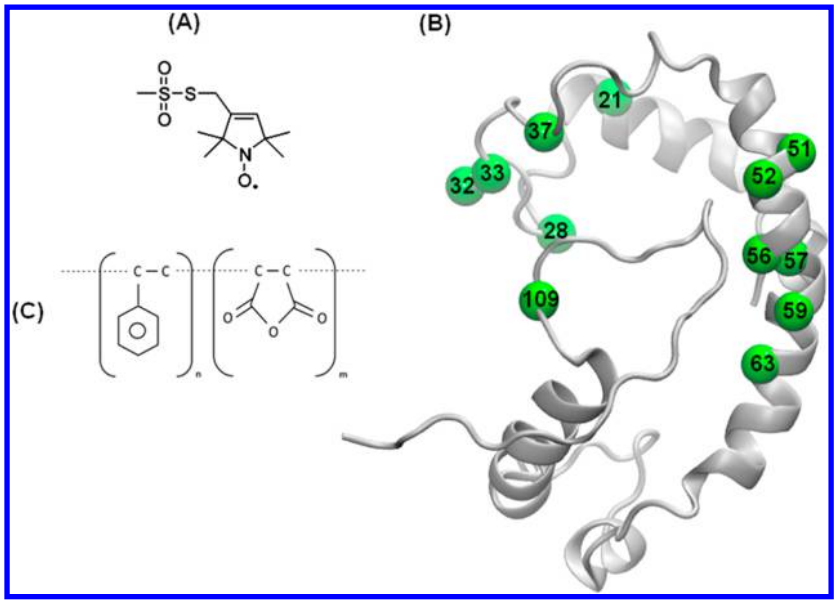


**Figure 1.** Chemical structure of the MTSL spin label probe (A), cartoon representation of the NMR structure of KCNE1 (PDB ID: 2k21) with spin-labeling sites represented by green spheres at their alpha carbons (B), and chemical structure of the 3:1 SMA polymer (C).

polymer 3:1 ratio) were purchased from Malvern Cosmeceutics Ltd. (Worcester, U.K.). The protein−lipid complex was incorporated into SMA−lipodisq nanoparticles following the published protocols.[7,15,24] A 500 $\mu$L aliquot of proteoliposome-reconstituted protein sample (~30 mM POPC/POPG lipid) was added with an increasing amount of 2.5% of lipodisq solution prepared in the same dialysis buffer (10 mM IMD, 0.1 mM EDTA at pH 6.5) dropwise over 3−4 min at different weight ratios (lipid:polymer = 1:0, 1:0.125, 1;0.25, 1:0.5, 1:0.75, 1:1, 1:2). The protein−lipodisq solution was allowed to equilibrate overnight at 4 °C.

**EPR Spectroscopic Measurements.** EPR experiments were conducted at the Ohio Advanced EPR Laboratory. CW-EPR spectra were collected at X-band on a Bruker EMX CW-EPR spectrometer using an ER041xG microwave bridge and ER4119-HS cavity coupled with a BVT 3000 nitrogen gas temperature controller. Each spin-labeled CW-EPR spectrum was acquired by signal averaging 10 42 s field scans with a central field of 3315 G and sweep width of 100 G, modulation frequency of 100 kHz, modulation amplitude of 1 G, and microwave power of 10 mW at 297 K. The side chain mobility was determined by calculating the inverse central line width from each CW EPR spectrum. Transverse relaxation data were collected by using a standard Hahn echo pulse sequence $[(\pi/2) - \tau_1 - (\pi) - \tau_1 - \text{echo}]$ at Q-band with 10/20 ns pulse widths, an initial $\tau_1$ of 200 ns and an increment of 16 ns, 100 echoes/point, and two-step phase cycling at 80 K. The transverse relaxation time ($T_2$) or phase memory time ($T_m$) was determined by fitting the data with a single exponential decay.

**EPR Spectral Simulations.** EPR spectra were simulated using the Multicomponent LabVIEW program written by Dr. Christian Altenbach[36] including the macroscopic order, microscopic disorder (MOMD) model developed by Freed group.[37,38] A previously published fitting procedure was used to simulate the CW-EPR spectra.[39] The principle components of the hyperfine interaction tensor **A** = [5.5 G, 5.5 G, 34.8 G] and **g**-tensors **g** = [2.0088, 2.0063, 2.0023] were obtained from our previously published work.[39] During the simulation process, the **A** and **g** tensors were held constant and the rotational diffusion tensors were varied. A two-site fit was used to account for both the rigid/slower and higher/faster motional components of the EPR spectrum. The best fit rotational correlation times and relative population of both components were determined using the Brownian diffusion model.

## RESULTS

Recently, we characterized the structure of lipodisq nanoparticles in the absence and in the presence of membrane protein KCNE1 using dynamic light scattering (DLS), solid state nuclear magnetic resonance (SSNMR) spectroscopy, and transmission electron microscopy (TEM).[40−42] In this study, the lipodisq nanoparticle system was characterized using a spin-labeled KCNE1 reconstituted into POPC/POPG lipid bilayers using CW-EPR line shape analysis, pulsed EPR phase memory time ($T_m$) measurements, and side-chain mobility analysis for spin-labeled sites inside and outside of the membrane. A POPC:POPG (3:1) lipid bilayer was used to mimic phospholipids typically found in mammalian membranes.[24,27,34,43] Figure 1 shows the schematic representation of the MTSL spin-label probe and the locations of the spin-labels mapped onto the NMR structure of the KCNE1 membrane protein in LMPG micelles.[25]

**CW-EPR Spectral Lineshape Analysis of KCNE1 in Lipodisq Nanoparticles.** CW-EPR spectra are very sensitive to the nitroxide side-chain motion of spin-labeled proteins incorporated into different environments (i. e., aqueous and membrane).[3,4] Important dynamic information can be gleaned from the EPR spectra. CW-EPR spectral line shape analysis was conducted on spin-labeled KCNE1 incorporated into POPC/POPG lipid bilayers upon titration of the SMA polymer. KCNE1 residues were chosen inside (F56C) and outside (R32C) of the membrane for these studies (Figure 1). F56C is buried in a hydrophobic lipid bilayer environment, while the R32C is outside of the membrane in an aqueous environment.[39] Figure 2 shows CW-EPR spectra of POPC/POPG vesicles titrating with 3:1 SMA polymers for spin-labeled R32C KCNE1 located outside the membrane at 297 and 318 K. The data reveal two motional components (slower/rigid component


DOI: 10.1021/acs.jpcb.7b01705
J. Phys. Chem. B 2017, 121, 5312−5321

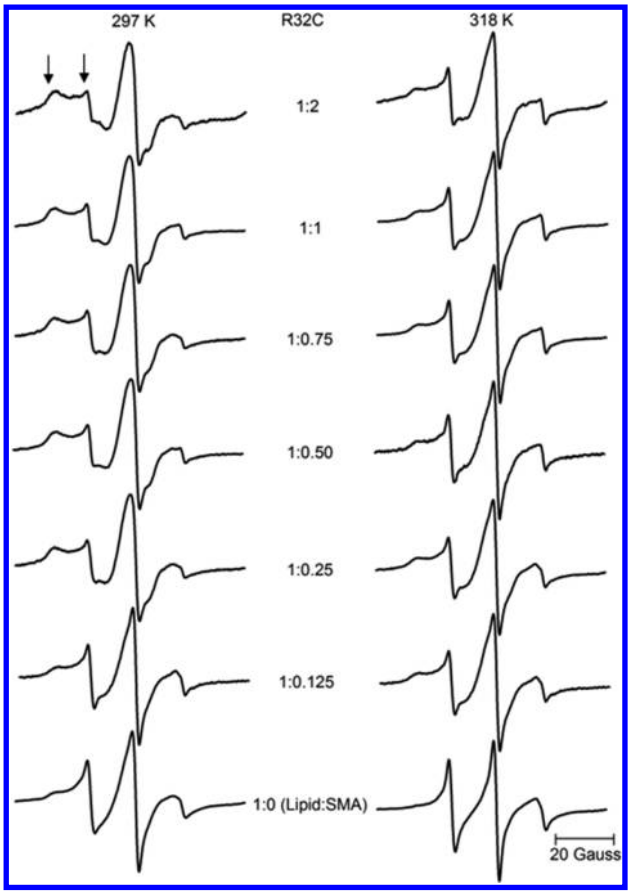


**Figure 2.** CW-EPR titration data on R32C-KCNE1 mutant (outside probe) in POPC/POPG vesicles as a control and lipodisq nanoparticles formed from different lipid to SMA polymer weight ratios as indicated in the corresponding spectrum.

indicated by left arrow and faster motional component indicated by right arrow) in the CW-EPR spectrum of the control sample (lipid:SMA polymer = 1:0) at 297 K. With the addition of the SMA polymer, the slower/rigid component (left peak) increases and the faster motional component (right peak) decreases and becomes a minimum and then saturates at a weight ratio of ∼1:1 W/W at 297 K. The slower component (left peak) is not so pronounced in the CW-EPR spectrum of the control sample (lipid:SMA polymer = 1:0) at 318 K. Upon addition of SMA polymer, CW-EPR spectra show two motional components (slower/rigid component (left peak) and faster motional component (right peak)). The slower/rigid component does not increase significantly with the addition of further SMA polymer. Inspection of the CW-EPR spectra indicates that the line shape broadening increases with the addition of the SMA polymer and becomes maximum and then saturates at a weight ratio of ∼1:1 W/W at 297 K. A single component EPR spectral line shape observed at 318 K for the control sample (lipid:SMA polymer = 1:0) might be due to the averaging of the two motional components at 318 K.[44] The other possible reason may be that the effect of viscosity will be less at 318 K for the sites located in the aqueous phase protecting to resolve the local motion contributing to the global motion in the resulting EPR spectrum.[7,15] The slower component observed in other spectra with the addition of SMA polymer is due to the residual slower component that was not fully averaged at 318 K. In order to compare the spectral line shape more quantitatively, the inverse central line widths obtained from all of the titration spectra (Figure 3) were plotted at temperatures of 297 and 318 K. The inverse central line width provides a quantitative

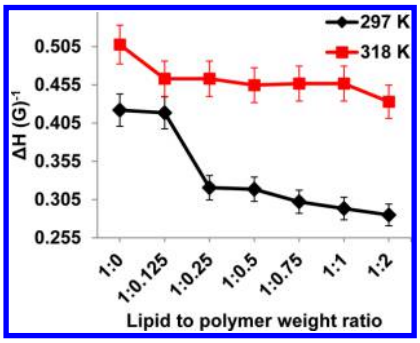


**Figure 3.** Side-chain mobility of the MTSL spin-label on KCNE1 at the R32C position (outside probe) for lipodisq nanoparticles formed from different lipid to SMA polymer weight ratios. The inverse central line width parameters were calculated from the CW-EPR titration spectra from Figure 2.

measure of the side-chain mobility of the spin-labeling sites.[5,39,45−47] The inverse central line width for the titration spectra at 297 K decreases from 1:0.125 to 1:0.25 weight ratios and then slows down and saturates at 1:1 and 1:2 weight ratios, while there is not significant variation in the inverse central line width at 318 K.

In order to further quantify the two motional components of the CW-EPR spectra, nonlinear least-squares (NLSL) MOMD EPR spectral simulations were carried out on representative EPR spectra of site R32C for the control sample (lipid:SMA polymer = 1:0) and for the sample in liposomes with the SMA polymer (lipid:SMA polymer = 1:1) to determine the correlation times and relative population of the different components. The multicomponent LabVIEW program developed by Christian Altenbach (http://www.biochemistry.ucla.edu/biochem/Faculty/Hubbell/) was used for the study.[36−38] The Zeeman interaction tensors ($\mathbf{g}_{xx}$, $\mathbf{g}_{yy}$, $\mathbf{g}_{zz}$) and hyperfine interaction tensors ($\mathbf{A}_{xx}$, $\mathbf{A}_{yy}$, $\mathbf{A}_{zz}$) were held constant during the fitting process, and the correlation times and relative population of the two components were determined from the best fit EPR spectra (see Figure S2). The simulation results indicated that the R32C KCNE1 mutant at a weight ratio of 1:1 is slower with longer correlation times of 7 ns and a relative population of 90% (rigid component) and 0.8 ns of 10% (motional component), and 6 ns with a relative population of 24% (rigid component) and 0.9 ns of 76% (motional component) for the control sample at a weight ratio of 1:0. These results are consistent with the previously published literature.[39]

Similarly, CW-EPR titration spectra of spin-labeled F56C located in the transmembrane domain of KCNE1 at temperatures of 297 and 318 K are shown in Figure 4. These CW-EPR spectra also reveal two motional components (slower/rigid component indicated by left arrow and faster motional component indicated by right arrow) in the control sample (lipid:SMA polymer = 1:0) at 297 K. The addition of the SMA polymer increases the slower/rigid component (left peak), while the faster motional component (right peak) decreases and becomes a minimum and then saturates at a weight ratio of ∼1:0.75 W/W at 297 K. The slower component (left peak) is not so pronounced in the CW-EPR spectrum of the control sample (lipid:SMA polymer = 1:0) at 318 K. The CW-EPR spectra also reveal two motional components (slower/rigid


DOI: 10.1021/acs.jpcb.7b01705
J. Phys. Chem. B 2017, 121, 5312−5321

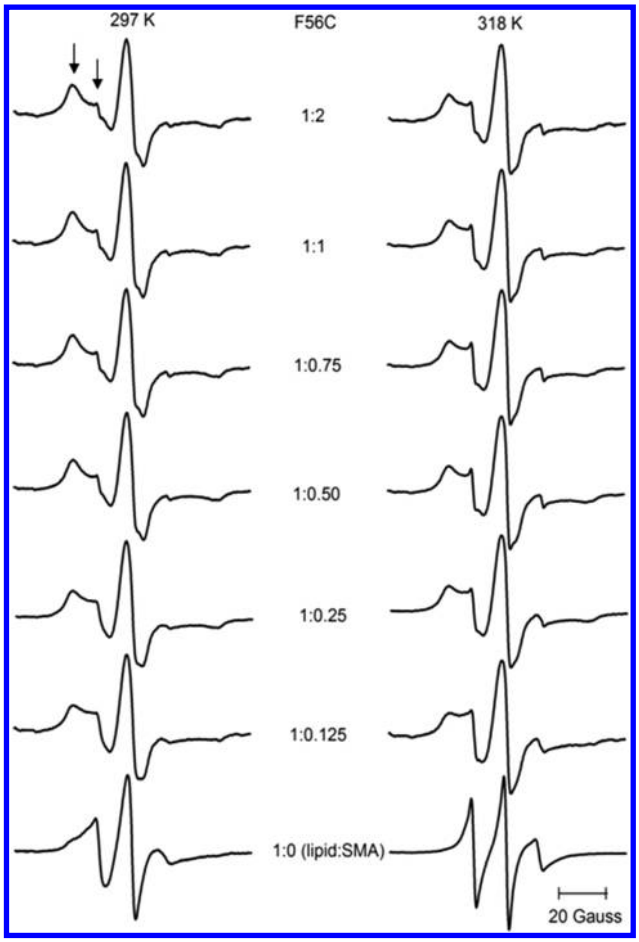


**Figure 4.** CW-EPR titration data on F56C-KCNE1 mutant (inside probe) in POPC/POPG vesicles as a control and lipodisq nanoparticles formed from different lipid to SMA polymer weight ratios as indicated in the corresponding spectrum.

component (left peak) and faster motional component (right peak)) upon addition of the SMA polymer. The slower/rigid component (left peak) increases significantly and the faster motional component (right peak) decreases with further addition of the SMA polymer and becomes minimum and then saturates at a weight ratio of ~1:0.75 W/W at 318 K. Inspection of the data indicates that the line width broadening increases with the addition of the SMA polymer and becomes maximum and then saturates at a weight ratio of ~1:0.75 W/W at both 297 and 318 K. A single component EPR spectral line shape observed at 318 K for the control sample (lipid:SMA polymer = 1:0) might be due to the averaging of the two motional components at 318 K, when compared to the spectra collected at 297 K. The other possible reason may be that the POPC/POPG lipid adopts a liquid phase at 318 K so that the lipid acyl chains have high fluidity, causing less restrictions to the spin label sites located inside the membrane averaging the overall motion of the spin label resulting in a single spectral component.[48] The overall spectral line broadening is higher for the inside transmembrane F56C KCNE1 sample, when compared to the spectra for the outside mutant R32C. The inverse central line width of spin-label mutant F56C (Figure 5) has a similar pattern to that of R32C. The inverse central line width values are lower, indicating that the EPR spectra are broader for F56C when compared to R32C. Figure 5 also revealed that there is a rapid decrease in inverse central line

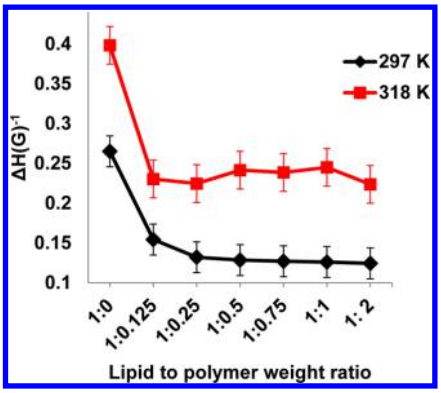


**Figure 5.** Side-chain mobility of the MTSL spin-label on KCNE1 at the F56C position (inside probe) for lipodisq nanoparticles formed from different lipid to SMA polymer weight ratios. The inverse central line width parameters were calculated from the CW-EPR titration spectra from Figure 4.

width for the F56C KCNE1 samples at weight ratios from 1:0 to 1:0.25 W/W. A significant increase in line broadening of the EPR spectrum causes the inverse central line width to decrease. The significant increase in line broadening observed for the inside probe F56C at 1:0.25 may be due to the higher restriction provided by the lipid acyl chain due to wrapping of the SMA polymer around the lipid bilayers while forming the lipodisq nanoparticle complex.[7,15,24] The CW-EPR titration spectra clearly indicate the spin-label motion gets slower with the addition of SMA polymer for both inside and outside mutants at 297 K. This behavior is not similar at 318 K. At 318 K, membrane fluidity is higher which can apply less restriction to the spin-label side-chain incorporated into the lipid bilayered vesicles, causing higher spin-label side-chain mobility of KCNE1 for the inside probe (F56C) when compared to that at 297 K.[48]

**Phase Memory Time ($T_m$) Measurements of KCNE1 in Lipodisq Nanoparticles.** Pulsed electron−electron double resonance (PELDOR)/double electron−electron resonance (DEER) spectroscopy coupled with SDSL is a powerful approach for measuring long-range distances of 18−80 Å,[4,24,49−51] and relative orientations,[52−54] providing valuable information for structural studies.[55,56] However, the application of DEER spectroscopy to spin-labeled membrane proteins in a reconstituted system is limited due to the much shorter phase memory times ($T_m$) of spin-labels in lipid bilayered vesicles[53,57−60] as compared to detergent micelles. The short phase memory times are due to uneven packing of the spin-labeled protein within the proteoliposomes, which creates local inhomogeneous pockets of high spin concentrations.[51] Homogeneous lipid bilayered vesicle sample preparation is required to enhance the phase memory time ($T_m$). In order to characterize lipodisq nanoparticles for pulsed EPR studies, we performed pulsed EPR titration experiments on outside and inside probes of KCNE1 (R32C and F56C) reconstituted into POPC/POPG liposomes with the addition of SMA polymer for the measurement of phase memory times ($T_m$). Figure 6 shows all of the $T_m$ curves for the R32C (outside, left panel) and F56C (transmembrane, right panel). The $T_m$ data were analyzed in a similar manner previously reported in the literature.[24] Figure 6 clearly indicates that the signal intensity at a specific decay time of 2 $\mu$s (DEER detectable time commonly used for biological systems) for the outside probe (R32C) is ~0.2 au for the control sample (POPC/POPG:SMA polymer =


DOI: 10.1021/acs.jpcb.7b01705
J. Phys. Chem. B 2017, 121, 5312−5321

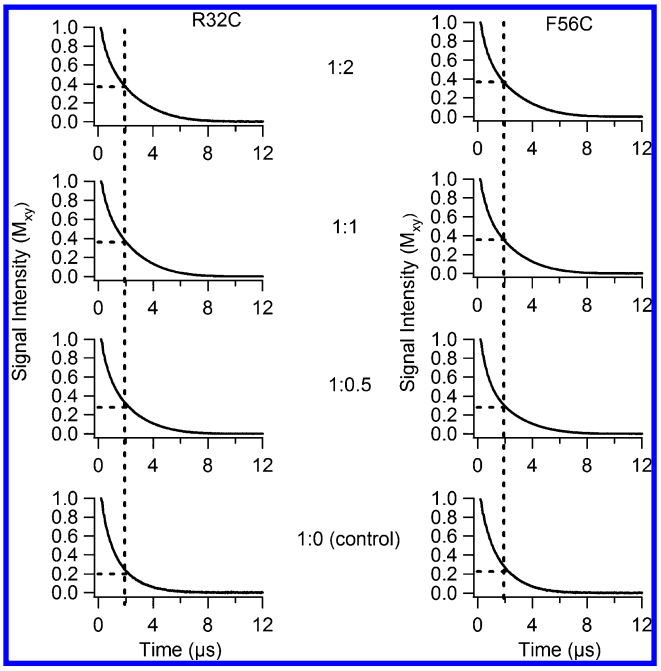


**Figure 6.** Phase memory time measurements on outside probe R32C-KCNE1 mutant (left panel) and inside probe F56C-KCNE1 mutant (right panel) reconstituted into POPC/POPG with addition of an increasing amount of 3:1 SMA polymer (lipid to polymer weight ratio) for the lipodisq nanoparticles. The phase memory time ($T_m$) values are similar for both inside and outside probes. The $T_m$ values are 1.4 ± 0.2 $\mu$s for 1:0, 1.8 ± 0.2 $\mu$s for 1:0.5, 1.9 ± 0.2 $\mu$s for 1:1, and 2.0 ± 0.2 $\mu$s for 1:2.

1:0). The addition of the SMA polymer to the sample significantly increases the signal amplitude up to ~0.4 au at 2 $\mu$s and saturates at a weight ratio of 1:2 W/W for the outside probe (R32C). These results indicate that the improvement in the transverse signal intensity observed is ~2-fold for the outside probe (R32C). Similarly, the signal intensity at a specific decay time of 2 $\mu$s (DEER detectable time commonly used for biological systems) for the inside probe (F56C) is ~0.2 au for the control sample (POPC/POPG:SMA polymer = 1:0). Addition of the SMA polymer increases the signal up to ~0.4 au and saturates at a weight ratio of 1:2 W/W for the inside probe (F56C). This is an ~2-fold increase, which is similar to the outside probe (R32C). All of the data sets could not be adequately fit with a single exponential decay to directly compare $T_m$ values for the different samples. However, qualitatively, the $T_m$ values of the outside probe (R32C) and inside probe (F56C) of KCNE1 for the control samples (POPC/POPG:SMA polymer = 1:0) were similar to the value of ~1.4 $\mu$s. The $T_m$ values increased up to ~2 $\mu$s at a weight ratio of 1:2 W/W for both outside and inside spin-label probes of KCNE1 (R32C and F56C) upon addition of the SMA polymer. The data indicate that the KCNE1 $T_m$ values can be improved by ~2-fold in lipodisq nanoparticles when compared to the same spin-labeled KCNE1 protein in proteoliposomes. With the improvement in the phase memory time, DEER measurements can be extended for a longer range of distances with higher signal-to-noise ratio (S/N) of the time domain DEER data.

**CW-EPR Spectral Measurements on inside Spin-Label Probes and outside Spin-Label Probes of KCNE1.** In order to further characterize the usage of lipodisq nanoparticles for EPR spectroscopic experiments, the CW-EPR line shape analysis and side-chain mobility of six inside and six outside MTSL spin-labeled mutants of KCNE1 were studied. Figure 7

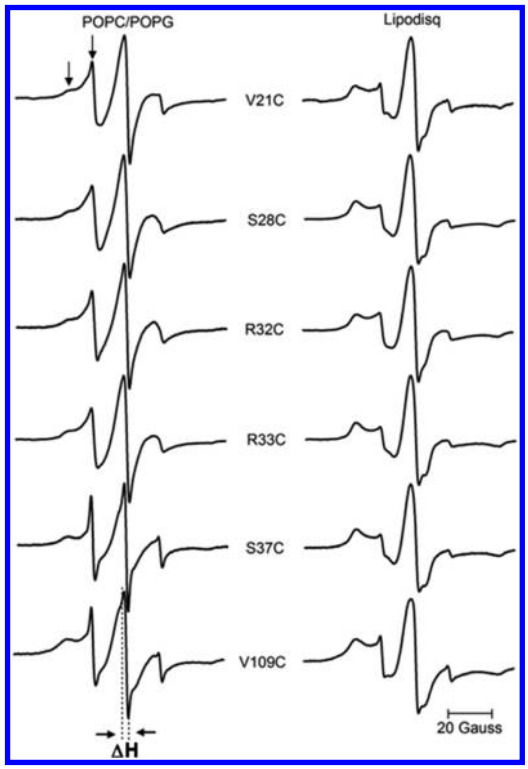


**Figure 7.** CW-EPR spectra on different outside mutants of KCNE1 in POPC/POPG vesicles and POPC/POPG lipodisq nanoparticles (lipid to polymer weight ratio = 1:1) at 297 K. $\Delta H$ represents the measurement of central line width.

shows CW-EPR spectra of the outside probes of the spin-labeled KCNE1 mutants in POPC/POPG liposomes and POPC/POPG lipodisq nanoparticles (lipid to SMA polymer weight ratio = 1:1) at 297 K. CW-EPR spectra reveal that the lipodisq nanoparticle samples have broader lineshapes closer to the rigid limit when compared to the POPC/POPG vesicle samples. The results also reveal two motional components in a majority of the EPR spectra. The left arrow shows the slower/rigid component and the right arrow shows faster motional components. These motional components arise due to the multiple conformational states of KCNE1 while interacting with the lipid bilayers.[39] The presence of multiple conformations of the spin-label rotamers and backbone fluctuation of KCNE1 may also contribute toward these two motional components.[61] The inverse central line width represents the spin-label side-chain mobility of membrane proteins that mostly contributed from the faster motional components of EPR spectra. The inverse central line width profile of the outside probes of KCNE1 (see Figure 8) for lipid bilayered vesicle samples is higher than that for the lipodisq nanoparticle samples. The inverse central line width values are between 0.37 andto0.53 $G^{-1}$ for vesicle samples and between 0.25 and 0.29 $G^{-1}$ for lipodisq nanoparticle samples. The CW-EPR spectra of transmembrane (inside) spin-labeled residues of KCNE1 (Figure 9) indicate that the lipodisq nanoparticle samples have significantly broader lineshapes when compared to that of vesicle samples. The inverse central line width profile of the inside probes of KCNE1 (see Figure 10) for vesicle samples is significantly higher than that for the lipodisq nanoparticle


DOI: 10.1021/acs.jpcb.7b01705
J. Phys. Chem. B 2017, 121, 5312−5321

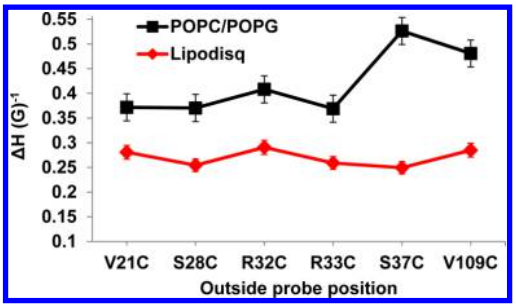


**Figure 8.** Inverse central line width as a function of outside probe positions of KCNE1 in POPC/POPG vesicles and POPC/POPG lipodisq nanoparticles (lipid to polymer weight ratio = 1:1). The inverse central line widths were calculated from the EPR spectra in Figure 7.

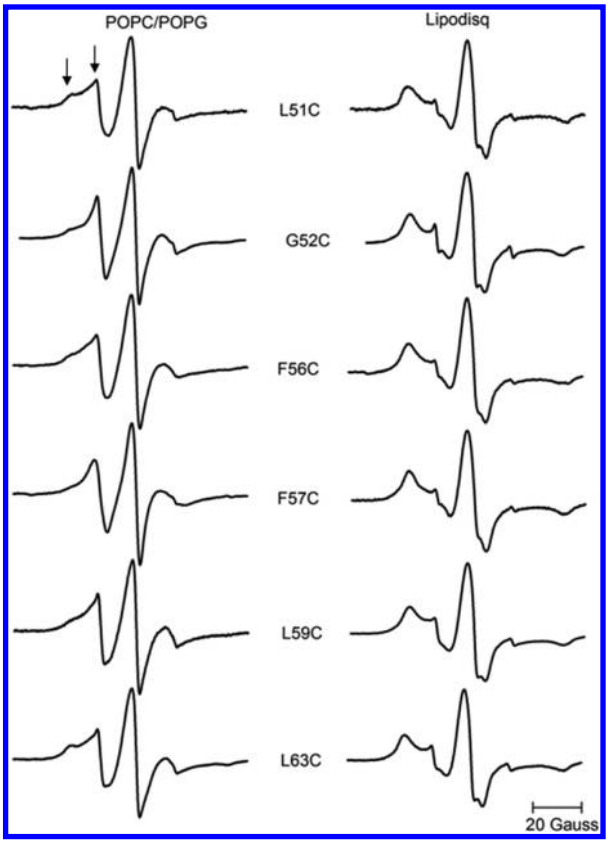


**Figure 9.** CW-EPR spectra on different inside mutants of KCNE1 in POPC/POPG vesicles and POPC/POPG lipodisq nanoparticles (lipid to polymer weight ratio = 1:1) at 297 K.

samples. The inverse central line width values are between 0.28 and 0.36 $G^{-1}$ for vesicle samples and between 0.12 and 0.14 $G^{-1}$ for lipodisq nanoparticles. Comparison of CW-EPR spectra and inverse central line widths of outside and inside spin-label probes of KCNE1 (Figures 7, 8, 9, and 10) reveal significant differences in line widths and mobilities for lipodisq nanoparticle samples. However, the spectral line widths and mobilities of inside probes and outside probes have smaller differences for the KCNE1 vesicle samples. The inside probes of KCNE1 have significantly broader spectral lineshapes and lower inverse central line widths when compared to outside probes of KCNE1. These results are expected as the KCNE1 transmembrane domian spans the full width of the lipid bilayer while C- and N-termini are solvent exposed, suggesting the

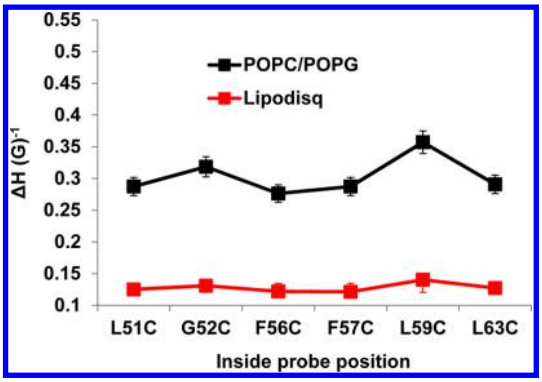


**Figure 10.** Inverse central line width as a function of inside probe positions of KCNE1 in POPC/POPG vesicles and POPC/POPG lipodisq nanoparticles (lipid to polymer weight ratio = 1:1). The inverse central line widths were calculated from the EPR spectra in Figure 9.

inside mutants tumble slower compared to the outside mutants of KCNE1.[39] The data indicate that CW-EPR spectra obtained in the lipodisq nanoparticles provide more obvious line broadening information for the faster motional components that the line broadening significantly increases for the residues located inside the membrane bilayers when compared to that of the residues located in the aqueous phase to understand the incorporation of KCNE1 in POPC/POPG liposomes. The data are consistent with our previously published structural topology model of KCNE1 in POPC/POPG lipid bilayered vesicles.[39]

## DISCUSSION

Homogeneous sample preparation is very important for obtaining high quality EPR data of membrane proteins for structural and dynamic studies. Our previous DEER data on several dual spin-labeled mutants of KCNE1 showed that the lipodisq based sample preparation provided significant improvement in signal-to-noise ratio (S/N) for DEER time domain data and boosted the phase memory time by ~2-fold.[24,35] CW-EPR titration data reported in this study indicate that the lipodisq nanoparticle system is optimum at the lipid to SMA polymer weight ratio of ~1:1 with a significant broadening in EPR spectral line shape. This spectral line shape broadening indicates that the spin-label motion is interestingly reduced for the lipodisq nanoparticle samples when compared to the proteoliposome samples. We speculate that this increase in line broadening may be related to the lipodisq nanoparticle formation mechanism, as suggested by previously published studies.[7,62,63] The additional EPR spectral line broadenings for the inside mutants might be due to a decrease in the motion of the lipid acyl chain in the presence of the SMA polymer while forming the lipodisq nanoparticles, resulting in a decrease in the motion of spin-labels. The lipodisq nanoparticle system is formed due to the lateral pressure generated due to the polymer and lipid chain interaction isolating the individual complex with specific smaller size.[7] Recent studies indicated that the SMA polymer forms like a bracelet around the lipid membrane with the styrene moieties oriented parallel to the membrane normal and interacting directly with the lipid acyl chain while maleic acid groups are oriented in the same direction of styrene moieties and interacting with the lipid head groups.[63] The driving force for the spontaneous formation of the lipodisq nanoparticles toward the burial of the styrene groups into the hydrophobic core of


DOI: 10.1021/acs.jpcb.7b01705
J. Phys. Chem. B 2017, 121, 5312−5321

the membrane might be contributing toward the decrease of lipid acyl chain motion. EPR experiments were also performed on the inside mutants (L48C, F56C) and outside mutant (L30C) of KCNE1 by removing the His-tag. The broadening of the EPR spectra is similar to and without the His-tag (see Supporting Information Figure S1). This indicates that the SMA polymer is not interacting with the His-tag while forming lipodisq nanoparticles. In the process of formation of the lipodisq nanoparticle systems, polymers extract the patches of membrane containing well incorporated membrane protein and stabilize the specific small sizes.[23] This may restrict the motion of lipid acyl chains and consequently may make the inside spin-label probes tumble slower compared to the liposome samples. In addition, the incorporation of a protein−lipid complex into the lipodisq nanoparticle system causes an overall increase in the viscosity of the solution slowing down the motion of the outside spin probe as well (see Figures 7 and 8).[7,15] Since the increase in viscosity causes a decrease in globular tumbling motion, the local motion of the spin-label caused by the lipid bilayers is clearly observed in the CW-EPR spectral line shape, causing inside spin-label probes with smaller inverse central line width when compared to that for outside spin-label probes (see Figures 7, 8, 9, and 10). This clearly differentiates the faster/higher motional components of spin-label for inside probes and outside probes of KCNE1 incorporated into POPC/POPG lipodisq nanoparticles.

Our previous DEER measurements indicated the most probable distances between the double mutants of KCNE1 were almost identical in POPC/POPG lipid bilayered vesicles and POPC/POPG lipodisq nanoparticles, suggesting that there is not significant structural perturbation on the protein due to lipodisq nanoparticle formation.[24,35] Recent studies have also reported that membrane proteins incorporated into lipodisq nanoparticles are still fully functional.[15,23] There is no direct restriction applied on membrane proteins due to the presence of the SMA polymer in lipodisq nanoparticles, and hence, the native membrane environment is preserved during biophysical measurements.[23] The overall reduction in the motion of the lipid−protein complex also helps to determine the local dynamics of spin probes.[64] The homogeneous formation of smaller sizes of lipodisq nanoparticles (containing one protein per particle on average) helps to evenly distribute the spin-labels, causing a decrease in the local spin concentration and increasing the phase memory time for DEER measurements.[15,24,35,42] Our previous DLS and TEM data suggested the optimized average sizes of lipodisq nanoparticles are 14−30 nm at the lipid to SMA polymer weight ratio of 1:1.25−1.5.[40,42] The optimized lipodisq nanoparticle based sample preparations reported in this study for the EPR spectroscopic studies are consistent with our previously optimized lipodisq nanoparticles for the SSNMR and TEM spectroscopic studies.[40,42] The transverse relaxation titration data showed that the phase memory time can be increased up to ∼2 $\mu$s with the addition of polymer at the weight ratio ∼1:1 for both inside and outside KCNE1 mutants (Figure 6). This indicates that the protein molecules are well isolated from each other due to smaller and homogeneous sizes of lipodisq nanoparticles. This enhancement in phase memory time is consistent with the previously published phase memory time of KCNE1 DEER samples in lipodisq nanoparticles.[24,35] However, the $T_m$ values for both inside and outside probes studied here are ∼1.4 $\mu$s for the vesicle samples which are larger than the ∼1 $\mu$s for DEER double mutants in vesicle samples.[24,35] This improvement may be due to the decrease in the local spin concentration in the case of single mutant samples used in this study. The increase in EPR spectral line broadening and phase memory time enhancement in lipodisq nanoparticle samples observed in this study are consistent with the KCNE1 protein reconstituted into POPC/POPG vesicles.[39] However, the spectral line broadenings and increase in $T_m$ values may vary depending upon the membrane protein systems, and the length and choice of phospholipids used for the study.[65] We speculate that the lipodisq nanoparticle system is potentially a good membrane mimetic and helpful for EPR studies of membrane proteins. However, further protein systems and lipid systems need to be examined to generalize the optimum benefit of using lipodisq nanoparticle based samples.

## CONCLUSION

Spin-labeled KCNE1 embedded inside lipodisq nanoparticles was characterized using CW and pulsed EPR spectroscopy. The EPR titration data indicated that the KCNE1 CW-EPR spectral line broadening increases with the addition of the SMA polymer to form lipodisq nanoparticles. Similarly, the transverse relaxation titration experiment indicated an increase in $T_m$ values upon addition of the SMA polymer. The CW-EPR spectral line shape analysis indicated significant differences in the faster components of spin-label side-chain mobilities between inside and outside probes of KCNE1. The enhancement in the $T_m$ value allows longer DEER distances to be measured more precisely for pertinent structural studies of challenging membrane protein systems. This lipodisq nanoparticle solubilization method can also be used for a variety of different lipid compositions. This study suggests that lipodisq nanoparticles can be used as a potentially good membrane mimic system to advance EPR studies of challenging membrane proteins for answering structure and dynamics related questions.

## ASSOCIATED CONTENT

### Supporting Information

The Supporting Information is available free of charge on the ACS Publications website at DOI: 10.1021/acs.jpcb.7b01705.

Additional CW data on KCNE1 with and without His-tag (Figure S1) and NLSL MOMD simulation of representative CW-EPR spectra (Figure S2) (PDF)

## AUTHOR INFORMATION


### Corresponding Author

*E-mail: gary.lorigan@miamioh.edu.

### ORCID

Gary A. Lorigan: 0000-0002-2395-3459


### Notes

The authors declare no competing financial interest.

## ACKNOWLEDGMENTS

This work was supported by National Institutes of Health Grants R01 GM108026. Funding was also provided by National Science Foundation (NSF) Grant CHE-1305664.

## REFERENCES

(1) Overington, J. P.; Al-Lazikani, B.; Hopkins, A. L. How many drug targets are there? *Nat. Rev. Drug Discovery* **2006**, *5*, 993−996.



DOI: 10.1021/acs.jpcb.7b01705
J. Phys. Chem. B 2017, 121, 5312−5321

(2) Sanders, C. R.; Myers, J. K. Disease-related misassembly of membrane proteins. *Annu. Rev. Biophys. Biomol. Struct.* **2004**, *33*, 25−51.
(3) Klug, C. S.; Feix, J. B. Methods and applications of site-directed spin labeling EPR spectroscopy. *Methods Cell Biol.* **2008**, *84*, 617−658.
(4) Sahu, I. D.; McCarrick, R. M.; Lorigan, G. A. Use of electron paramagnetic resonance to solve biochemical problems. *Biochemistry* **2013**, *52*, 5967−5984.
(5) Hubbell, W. L.; McHaourab, H. S.; Altenbach, C.; Lietzow, M. A. Watching proteins move using site-directed spin labeling. *Structure* **1996**, *4*, 779−783.
(6) Zou, P.; McHaourab, H. S. Increased sensitivity and extended range of distance measurements in spin-labeled membrane proteins: Q-band double electron-electron resonance and nanoscale bilayers. *Biophys. J.* **2010**, *98*, L18−L20.
(7) Orwick, M. C.; Judge, P. J.; Procek, J.; Lindholm, L.; Graziadei, A.; Engel, A.; Grobner, G.; Watts, A. Detergent-free formation and physicochemical characterization of nanosized lipid-polymer complexes: lipodisq. *Angew. Chem., Int. Ed.* **2012**, *51*, 4653−4657.
(8) Lau, T.-L.; Kim, C.; Ginsberg, M. H.; Ulmer, T. S. The structure of the integrin alpha IIb beta 3 transmembrane complex explains integrin transmembrane signalling. *EMBO J.* **2009**, *28*, 1351−1361.
(9) Lee, D.; Walter, K. F. A.; Brueckner, A.-K.; Hilty, C.; Becker, S.; Griesinger, C. Bilayer in small bicelles revealed by lipid-protein interactions using NMR spectroscopy. *J. Am. Chem. Soc.* **2008**, *130*, 13822−13823.
(10) Sanders, C. R.; Prosser, R. S. Bicelles: a model membrane system for all seasons? *Structure* **1998**, *6*, 1227−1234.
(11) Lu, Z.; Van Horn, W. D.; Chen, J.; Mathew, S.; Zent, R.; Sanders, C. R. Bicelles at low concentrations. *Mol. Pharmaceutics* **2012**, *9*, 752−761.
(12) Raschle, T.; Hiller, S.; Etzkorn, M.; Wagner, G. Nonmicellar systems for solution NMR spectroscopy of membrane proteins. *Curr. Opin. Struct. Biol.* **2010**, *20*, 471−479.
(13) Vold, R. R.; Prosser, R. S. Magnetically oriented phospholipid bilayered micelles for structural studies of polypeptides. Does the ideal bicelle exist? *J. Magn. Reson., Ser. B* **1996**, *113*, 267−271.
(14) Duerr, U. H. N.; Gildenberg, M.; Ramamoorthy, A. The magic of bicelles lights up membrane protein structure. *Chem. Rev.* **2012**, *112*, 6054−6074.
(15) Orwick-Rydmark, M.; Lovett, J. E.; Graziadei, A.; Lindholm, L.; Hicks, M. R.; Watts, A. Detergent-free incorporation of a seven-transmembrane receptor protein into nanosized bilayer lipodisq particles for functional and biophysical studies. *Nano Lett.* **2012**, *12*, 4687−4692.
(16) Knowles, T. J.; Finka, R.; Smith, C.; Lin, Y.-P.; Dafforn, T.; Overduin, M. Membrane proteins solubilized intact in lipid containing nanoparticles bounded by styrene maleic acid copolymer. *J. Am. Chem. Soc.* **2009**, *131*, 7484−7485.
(17) Jamshad, M.; Lin, Y.-P.; Knowles, T. J.; Parslow, R. A.; Harris, C.; Wheatley, M.; Poyner, D. R.; Bill, R. M.; Thomas, O. R. T.; Overduin, M.; Dafforn, T. R. Surfactant-free purification of membrane proteins with intact native membrane environment. *Biochem. Soc. Trans.* **2011**, *39*, 813−818.
(18) Dorr, J. M.; Scheidelaar, S.; Koorengevel, M. C.; Dominguez, J. J.; Schafer, M.; van Walree, C. A.; Killian, J. A. The styrene-maleic acid copolymer: a versatile tool in membrane research. *Eur. Biophys. J.* **2016**, *45*, 3−21.
(19) Gulati, S.; Jamshad, M.; Knowles, T. J.; Morrison, K. A.; Downing, R.; Cant, N.; Collins, R.; Koenderink, J. B.; Ford, R. C.; Overduin, M.; et al. Detergent-free purification of ABC (ATP-binding-cassette) transporters. *Biochem. J.* **2014**, *461*, 269−278.
(20) Shi, L.; Shen, Q.-T.; Kiel, A.; Wang, J.; Wang, H.-W.; Melia, T. J.; Rothman, J. E.; Pincet, F. SNARE proteins: one to fuse and three to keep the nascent fusion pore open. *Science* **2012**, *335*, 1355−1359.
(21) Scheidelaar, S.; Koorengevel, M. C.; Pardo, J. D.; Meeldijk, J. D.; Breukink, E.; Killian, J. A. Molecular model for the solubilization of membranes into nanodisks by styrene maleic acid copolymers. *Biophys. J.* **2015**, *108*, 279−290.
(22) Long, A. R.; O'Brien, C. C.; Malhotra, K.; Schwall, C. T.; Albert, A. D.; Watts, A.; Alder, N. N. A detergent-free strategy for the reconstitution of active enzyme complexes from native biological membranes into nanoscale discs. *BMC Biotechnol.* **2013**, *13*, 41.
(23) Logez, C.; Damian, M.; Legros, C.; Dupre, C.; Guery, M.; Mary, S.; Wagner, R.; M'Kadmi, C.; Nosjean, O.; Fould, B.; et al. Detergent-free isolation of functional g protein-coupled receptors into nanometric lipid particles. *Biochemistry* **2016**, *55*, 38−48.
(24) Sahu, I. D.; MaCarrick, R. M.; Troxel, K. R.; Zhang, R.; Smith, J. H.; Dunagan, M. M.; Swartz, M. S.; Rajan, P. V.; Kroncke, B. M.; Sanders, C. R.; et al. DEER EPR measurement for membrane protein structures via bifunctional spin labels and lipodisq nanoparticles. *Biochemistry* **2013**, *52*, 6627−6632.
(25) Kang, C.; Tian, C.; Sonnichsen, F. D.; Smith, J. A.; Meiler, J.; George, A. L. J.; Vanoye, C. G.; Kim, H. J.; Sanders, C. R. Structure of KCNE1 and implications for how it modulates the kcnq1potassium channel. *Biochemistry* **2008**, *47*, 7999−8006.
(26) Tian, C.; Vanoye, C. G.; Kang, C.; Welch, R. C.; Kim, H. J.; George, A. L.; Sanders, C. R. Preparation, functional characterization, and NMR studies of human KCNE1, a voltage-gated potassium channel accessory subunit associated with deafness and long QT syndrome. *Biochemistry* **2007**, *46*, 11459−11472.
(27) Coey, A. T.; Sahu, I. D.; Gunasekera, T. S.; Troxel, K. R.; Hawn, J. M.; Swartz, M. S.; Wickenheiser, M. R.; Reid, R. J.; Welch, R. C.; Vanoye, C. G.; et al. Reconstitution of KCNE1 into lipid bilayers: comparing the structural, dynamic, and activity differences in micelle and vesicle environments. *Biochemistry* **2011**, *50*, 10851−10859.
(28) Melman, Y. F.; Um, S. Y.; Krumerman, A.; Kagan, A.; McDonald, T. V. KCNE1 binds to the KCNQ1 pore to regulate potassium channel activity. *Neuron* **2004**, *42*, 927−937.
(29) Panaghie, G.; Tai, K. K.; Abbott, G. W. Interaction of KCNE subunits with the KCNQ1 K+ channel pore. *J. Physiol.* **2006**, *570*, 455−467.
(30) Li, G.-R.; Feng, J.; Yue, L.; Carrier, M.; Nattel, S. Evidence for two components of delayed rectifi er K + current in human ventricular myocytes. *Circ. Res.* **1996**, *78*, 689−696.
(31) Jost, N.; Virag, L.; Bitay, M.; Takacs, J.; Lengye, l. C.; Biliczki, P.; Nagy, Z.; Bogats, G.; Lathrop, D. A.; Papp, J. G.; et al. Restricting excessive cardiac action potential and QT prolongation. A vital role for I Ks in human ventricular muscle. *Circulation* **2005**, *112*, 1392−1399.
(32) Wang, Z.; Fermini, B.; Nattel, S. Rapid and slow components of delayed rectifi er current in human atrial myocytes. *Cardiovasc. Res.* **1994**, *28*, 1540−1546.
(33) Harmer, S. C.; Tinker, A. The role of abnormal trafficking of KCNE1 in long QT syndrome 5. *Biochem. Soc. Trans.* **2007**, *35*, 1074−1076.
(34) Barrett, P. J.; Song, Y.; Van Horn, W. D.; Hustedt, E. J.; Schafer, J. M.; Hadziselimovic, A.; Beel, A. J.; Sanders, C. R. The amyloid precursor protein has a flexible transmembrane domain and binds cholesterol. *Science* **2012**, *336*, 1168−1171.
(35) Sahu, I. D.; Kroncke, B. M.; Zhang, R.; Dunagan, M. M.; Smith, H. J.; Craig, A.; McCarrick, R. M.; Sanders, C. R.; Lorigan, G. A. Structural investigation of the transmembrane domain of KCNE1 in proteoliposomes. *Biochemistry* **2014**, *53*, 6392−6401.
(36) Toledo Warshaviak, D.; Khramtsov, V. V.; Cascio, D.; Altenbach, C.; Hubbell, W. L. Structure and dynamics of an imidazoline nitroxide side chain with strongly hindered internal motion in proteins. *J. Magn. Reson.* **2013**, *232*, 53−61.
(37) Schneider, D. J.; Freed, J. H. Calculating slow motional magnetic resonance spectra: a user's guide. In *Biol. Magn. Reson.*; Berlinger, L. J., Ed.; Plenum Publishing: New York, 1989.
(38) Budil, D. E.; Lee, S.; Saxena, S.; Freed, J. H. Nonlinear-least-squares analysis of slow-motion EPR spectra in one and two dimensions using a modified levenberg−marquardt algorithm. *J. Magn. Reson., Ser. A* **1996**, *120*, 155−189.
(39) Sahu, I. D.; Craig, A. F.; Dunagan, M. M.; Troxel, K. R.; Zhang, R.; Meiberg, A. G.; Harmon, C. N.; MaCarrick, R. M.; Kroncke, B. M.; Sanders, C. R.; et al. Probing structural dynamics and topology of the kcne1 membrane protein in lipid bilayers via site-directed spin labeling


DOI: 10.1021/acs.jpcb.7b01705
*J. Phys. Chem. B* 2017, 121, 5312−5321

and electron paramagnetic resonance spectroscopy. *Biochemistry* **2015**, *54*, 6402−6412.
(40) Zhang, R.; Sahu, I. D.; Liu, L.; Osatuke, A.; Corner, R. G.; Dabney-Smith, C.; Lorigan, G. A. Characterizing the structure of lipodisq nanoparticles for membrane protein spectroscopic studies. *Biochim. Biophys. Acta, Biomembr.* **2015**, *1848*, 329−333.
(41) Craig, A. F.; Clark, E. E.; Sahu, I. D.; Zhang, R.; Frantz, N. D.; Al-Abdul-Wahid, S.; Dabney-Smith, C.; Konkolewicz, D.; Lorigan, G. A. Tuning the size of styrene-maleic acid copolymer-lipid nanoparticles (SMALPs) using RAFT polymerization for biophysical studies. *Biochim. Biophys. Acta, Biomembr.* **2016**, *1858*, 2931−2939.
(42) Zhang, R.; Sahu, I. D.; Bali, A. P.; Dabney-Smith, C.; Lorigan, G. A. Characterization of the structure of lipodisq nanoparticles in the presence of kcne1 by dynamic light scattering and transmission electron microscopy. *Chem. Phys. Lipids* **2017**, *203*, 19−23.
(43) Song, Y.; Hustedt, E. J.; Brandon, S.; Sanders, C. R. Competition between homodimerization and cholesterol binding to the C99 domain of the amyloid precursor protein. *Biochemistry* **2013**, *52*, 5051−5064.
(44) Ghimire, H.; Hustedt, E. J.; Sahu, I. D.; Inbaraj, J. J.; McCarrick, R.; Mayo, D. J.; Benedikt, M. R.; Lee, R. T.; Grosser, S. M.; Lorigan, G. A. Distance measurements on a dual-labeled toac achr m2$\delta$ peptide in mechanically aligned DMPC bilayers via dipolar broadening CW-EPR spectroscopy. *J. Phys. Chem. B* **2012**, *116*, 3866−3873.
(45) Hubbell, W. L.; Cafiso, D. S.; Altenbach, C. Identifying conformational changes with site-directed spin labeling. *Nat. Struct. Biol.* **2000**, *7*, 735−739.
(46) Hubbell, W. L.; Gross, A.; Langen, R.; Lietzow, M. A. Recent advances in site-directed spin labeling of proteins. *Curr. Opin. Struct. Biol.* **1998**, *8*, 649−656.
(47) Sahu, I. D.; Lorigan, G. A. Biophysical EPR studies applied to membrane proteins. *J. Phys. Chem. Biophys.* **2015**, *5*, 188.
(48) Fan, W.; Evans, R. M. Turning up the heat on membrane fluidity. *Cell* **2015**, *161*, 962−963.
(49) Borbat, P. P.; McHaourab, H. S.; Freed, J. H. Protein structure determination using long-distance constraints from double-quantum coherence ESR: study of T4 lysozyme. *J. Am. Chem. Soc.* **2002**, *124*, 5304−5314.
(50) Jeschke, G.; Polyhach, Y. Distance measurements on spin-labelled biomacromolecules by pulsed electron paramagnetic resonance. *Phys. Chem. Chem. Phys.* **2007**, *9*, 1895−1910.
(51) Jeschke, G. DEER distance measurements on proteins. *Annu. Rev. Phys. Chem.* **2012**, *63*, 419−446.
(52) Schiemann, O.; Cekan, P.; Margraf, D.; Prisner, T. F.; Sigurdsson, S. T. Relative orientation of rigid nitroxides by PELDOR: beyond distance measurements in nucleic acids. *Angew. Chem., Int. Ed.* **2009**, *48*, 3292−3295.
(53) Endeward, B.; Butterwick, J. A.; MacKinnon, R.; Prisner, T. F. Pulsed electron-electron double-resonance determination of spin-label distances and orientations on the tetrameric potassium ion channel KcsA. *J. Am. Chem. Soc.* **2009**, *131*, 15246−15250.
(54) Marko, A.; Margraf, D.; Cekan, P.; Sigurdsson, S. T.; Schiemann, O.; Prisner, T. F. Analytical method to determine the orientation of rigid spin labels in DNA. *Phys. Rev. E* **2010**, *81*, 021911−9.
(55) Jao, C. C.; Hegde, B. G.; Chen, J.; Haworth, I. S.; Langen, R. Structure of membrane-bound alpha-synuclein from site-directed spin labeling and computational refinement. *Proc. Natl. Acad. Sci. U. S. A.* **2008**, *105*, 19666−19671.
(56) Mokdad, A.; Herrick, D. Z.; Kahn, A. K.; Andrews, E.; Kim, M.; Cafiso, D. S. Ligand-induced structural changes in the escherichia coli ferric citrate transporter reveal modes for regulating protein-protein interactions. *J. Mol. Biol.* **2012**, *423*, 818−830.
(57) Jeschke, G.; Wegener, C.; Nietschke, M.; Jung, H.; Steinhoff, H. J. Interresidual distance determination by four-pulse double electron-electron resonance in an integral membrane protein: the Na+/proline transporter PutP of Escherichia coli. *Biophys. J.* **2004**, *86*, 2551−2557.
(58) Hilger, D.; Jung, H.; Padan, E.; Wegener, C.; Vogel, K. P.; Steinhoff, H. J.; Jeschke, G. Assessing oligomerization of membrane proteins by four-pulse DEER: pH-dependent dimerization of NhaA Na+/H+ antiporter of E-coli. *Biophys. J.* **2005**, *89*, 1328−1338.
(59) Hilger, D.; Polyhach, Y.; Padan, E.; Jung, H.; Jeschke, G. High-resolution structure of a Na+/H+ antiporter dimer obtained by pulsed election paramagnetic resonance distance measurements. *Biophys. J.* **2007**, *93*, 3675−3683.
(60) Xu, Q.; Ellena, J. F.; Kim, M.; Cafiso, D. S. Substrate-dependent unfolding of the energy coupling motif of a membrane transport protein determined by double electron-electron resonance. *Biochemistry* **2006**, *45*, 10847−10854.
(61) Altenbach, C.; Flitsch, S. L.; Khorana, H. G.; Hubbell, W. L. Structural studies on transmembrane proteins. 2. spin labeling of bacteriorhodopsin mutants at unique cysteines. *Biochemistry* **1989**, *28*, 7806−7812.
(62) Stepien, P.; Polit, A.; Wisniewska-Becker, A. Comparative EPR studies on lipid bilayer properties in nanodiscs and liposomes. *Biochim. Biophys. Acta, Biomembr.* **2015**, *1848*, 60−66.
(63) Jamshad, M.; Grimard, V.; Idini, I.; Knowles, T. J.; Dowle, M. R.; Schofield, N.; Sridhar, P.; Lin, Y.; Finka, R.; Wheatley, M.; et al. Structural analysis of a nanoparticle containing a lipid bilayer used for detergent-free extraction of membrane proteins. *Nano Res.* **2015**, *8*, 774−789.
(64) Fleissner, M. R.; Bridges, M. D.; Brooks, E. K.; Cascio, D.; Kálai, T.; Hideg, K.; Hubbell, W. L. Structure and dynamics of a conformationally constrained nitroxide side chain and applications in EPR spectroscopy. *Proc. Natl. Acad. Sci. U. S. A.* **2011**, *108*, 16241−16246.
(65) Kandasamy, S. K.; Larson, R. G. Molecular dynamics simulations of model trans-membrane peptides in lipid bilayers: a systematic investigation of hydrophobic mismatch. *Biophys. J.* **2006**, *90*, 2326−2343.


DOI: 10.1021/acs.jpcb.7b01705
*J. Phys. Chem. B* 2017, 121, 5312−5321